Chapter 12
Powering Fuel Cells Through Biocatalysis

Dónal Leech, Marie Pellissier and Frédéric Barrière

12.1. Introduction

Monitoring and control of a range of medical conditions will increasingly be performed by sophisticated, miniaturized, integrated implanted medical devices [1]. Provision of miniaturized, implantable power sources to drive these devices is therefore of significant importance. Current miniaturized battery technology uses highly reactive lithium, or corrosive alkaline electrolytes. This necessitates use of protective cases and seals to prevent leakage, making miniaturization expensive and difficult. Biocatalytic fuel cells have the potential to deliver a simple, inexpensive, miniaturized, implanted power supply [1-3].

Fuel cells generate electricity through an electrochemical process in which the energy stored in a fuel is converted directly into electricity. Fuel cells chemically combine the molecules of a fuel and oxidant, without burning, dispensing with the inefficiencies and pollution of traditional combustion.

In principle, a fuel cell operates like a battery. Unlike a battery, a fuel cell does not run down or require recharging: it will produce electricity as long as fuel and oxidant are supplied. The electrochemical reactions of a fuel cell consist of two separate reactions: an oxidation half-reaction occurring at the anode and a reduction half-reaction occurring at the cathode. The anode and the cathode are separated from each other by the electrolyte and an ion-exchange membrane. In the oxidation half-reaction, the input fuel passes over the anode and is catalytically split, producing ions, which travel through the electrolyte to the

cathode, and electrons, which travel through an external circuit to serve an electric load, which consumes the power generated, to the cathode. In the reduction half-reaction, an oxidant, supplied from air or fluid flowing past the cathode, combines with the ions and electrons to complete the circuit. The power output of the fuel cell is the product of the cell voltage and the cell current. The theoretical thermodynamic cell voltage is the difference in standard reduction potentials of the oxidant and fuel. System losses, however, in the form of kinetic and mass transport limitations and IR drop can severely lower the power output of fuel cells. For example, in commercial fuel cells, catalysts are used on both the anode and cathode to increase the kinetics of each half-reaction. The catalyst that works the best on each electrode is platinum, a non-selective catalyst, and a very expensive material.

Biocatalytic fuel cells are fuel cells which rely upon biocatalytic reactions at the electrodes to convert chemical fuels and oxidants into electrical power. The biocatalytic reactions used to produce power range from reactions of fermentation broths containing whole cells, to isolated enzyme biocatalysts. Fermentation broths containing microbial cells can be used to produce chemical fuels, such as sugars or hydrogen, in the anodic compartment of a fuel cell [2]. The production of the fuels from microbial cells by fermentation may alternatively be de-coupled from the fuel cell, with the fuel being fed into a conventional fuel cell [2]. Extraction of electrical power from microbial fermentation processes can also be by addition of small redox molecules that can mediate electron transfer from the microbial electron transport pathway to the electrode surface [2]. An advantage of using whole cells to produce power is that the biocatalysts and micro-organisms can be maintained in their natural environment, whilst efficiently producing power over long periods. The power densities that can be extracted from these fuel cells are, however, typically low, and they are thus expected to find limited application in implanted electronic devices. Renewed research in development of these types of fuel cells has instead been driven by the goal of large-scale clean power production. Given the low power densities of these cells, however, it is doubtful if this technology will ever compete with conventional fuel cells [3].

Biocatalytic fuel cells using isolated redox enzymes were first investigated in 1964 [4]. These fuel cells represent a more realistic opportunity for provision of implantable power, given the exquisite selectivity of enzyme catalysts, their activity under physiological conditions, and the relative ease of immobilization of isolated enzymes, compared to the microbial fuel cells. Implantable biocatalytic fuel cells have thus been proposed, where the body's own chemicals are used to produce power *in-vivo*.

In this chapter, progress on biocatalytic fuel cell research is reviewed. Particularly, reported biocatalytic fuel cell prototypes are critically assessed against the long term goal of the design of a small, implantable and long-lived, low-power source for biomedical applications. In this context, the substrates of choice to power such a device are free oxygen as the oxidant and glucose as the fuel, both present in significant concentration in physiological media. Although other recently reported biocatalytic fuel cells not exclusively relying on glucose or oxygen are of interest to the field, we will mainly focus on the glucose-oxygen system, with eventual implantation in mind.

The first oxygen-glucose biocatalytic fuel cell working at neutral pH was reported in 1964 [4]. The over-ambitious goal of the time was to power energy-demanding devices like the artificial heart. The development of the field occurred concomitantly with the

development of bioelectrochemistry [5]. The low current densities obtained in these early, and to some extent current, prototypes gradually re-oriented the biocatalytic fuel cell research towards more modest and sensible aims [1-3]. The recent upsurge in interest in biocatalytic fuel cell research is driven in part by the convergence of advances, on the one hand, in biosensor design and enzyme electrochemistry, particularly in terms of increasing stable current densities at modified electrodes, and on the other hand, in microelectronics, where ever smaller and lower-energy consuming devices are being manufactured. These advances now possibly make the implantable low-power biocatalytic fuel cell a realistic goal, although many issues still need to be resolved. Several interesting reviews on aspects of biocatalytic fuel cell research have appeared in the last decade [1-3,6,7]. Here, we review the development of this exciting research area, concentrating initially on some basic principles, then on the cathode compartment of the cell, then on the anode, and finally summarizing research on combining the two electrodes to provide prototype biocatalytic fuel cells.

12.2. Biocatalytic Fuel Cell Design

Contrary to traditional fuel cells, biocatalytic fuel cells are in principle very simple in design [1]. Fuel cells are usually made of two half-cell electrodes, the anode and cathode, separated by an electrolyte and a membrane that should avoid mixing of the fuel and oxidant at both electrodes, while allowing the diffusion of ions to/from the electrodes. The electrodes and membrane assembly needs to be sealed and mounted in a case from which plumbing allows the fuel and oxidant delivery to the anode and cathode, respectively, and exhaustion of the reaction products. In contrast, the simplicity of the biocatalytic fuel cell design rests on the specificity of the catalyst brought upon by the use of enzymes.

Provided that the required enzymes can be immobilized at, and electrically communicated with, the surface of an electrode, with retention of their high catalytic properties and there is no electrolysis of fuel at the cathode or oxidant at the anode, or a solution redox reaction between fuel and oxidant, the biocatalytic fuel cell then simply consists of the modified cathode and anode separated by an electrolyte containing both fuel and oxidant, connected to a load, as depicted in the schematic in Fig. 1. The design simplicity allows miniaturization of the cell. Realistic reachable power outputs, however, should restrict future devices to powering low-energy demanding systems.

12.3. Electron Transfer Reactions

Electronic communication between electrode surfaces and biocatalysts can be achieved by direct electron transfer if the active site of the biocatalyst is not located too remote from the protein surface, as discussed elsewhere in this book (chapter 17). Direct electron transfer is an attractive process for fuel cells as no other molecules except the substrate and the enzyme are involved in the electrocatalytic reaction, as depicted in the schematic in Fig. 2. The enzyme is the relay for the electron transfer between the substrate and the electrode surface. Recent advances in tailoring surface nano-structural features to match the size of co-substrate channels in biocatalysts, and in re-constituting active prosthetic groups tethered to, and communicating electronically with, surfaces, with apo-enzymes, are

elegant demonstrations of direct electron transfer to biocatalyst active sites that were previously considered inaccessible to electrode surfaces [8-17].

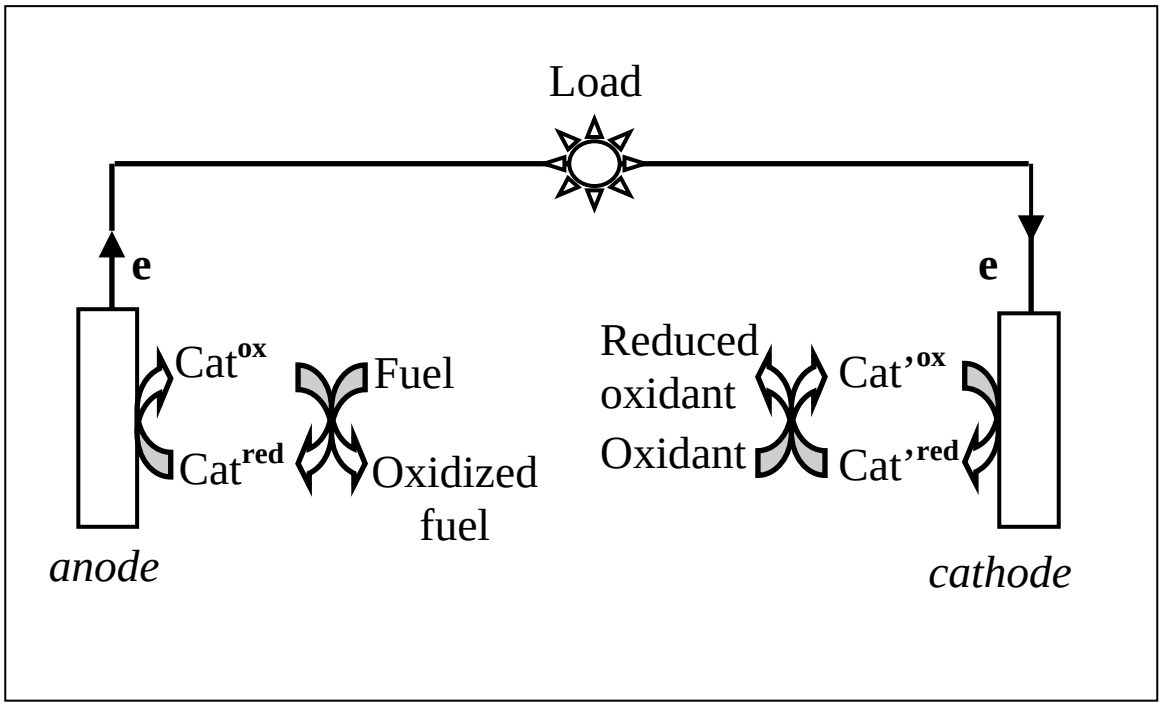

Fig. 1. Schematic depiction of a biocatalytic fuel cell, with fuel oxidation by a biocatalyst (Cat) at the anode and oxidant reduction by a biocatalyst (Cat') at the cathode, in a membraneless assembly, providing power to the load.

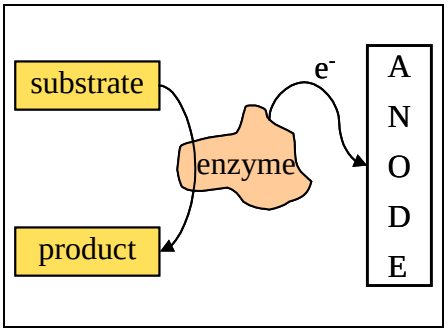

Fig. 2. Schematic depicting a direct electron transfer process between an enzyme and the electrode, acting as an anode in this case.

Current and power densities achieved with electrodes using the direct electron transfer approach will be limited, however, because of the need to have intimate contact between the two-dimensional electrode surface and a coating monolayer of correctly oriented biocatalyst. The use of small redox molecules that can mediate electron transfer between

the biocatalyst and the electrode surface offers an opportunity to improve output from biocatalytic electrodes, as three dimensional films of biocatalysts may now be used. In addition the distance between the active site of the enzyme and the electrode surface is often too great to allow efficient direct electron transfer. In these cases the electron transfer rate is not effective because of the insulation of the redox active site by the surrounding protein. A redox mediator can shuttle electrons between the enzyme and the surface. In the example of redox mediated biocatalytic oxidation of a fuel, depicted in Fig. 3, the enzyme catalyzes the oxidation of the mediator and the mediator is considered to be the second substrate (co-substrate) of the catalytic process. The use of mediators can increase the rate of electron transfer, sometimes by several orders of magnitude.

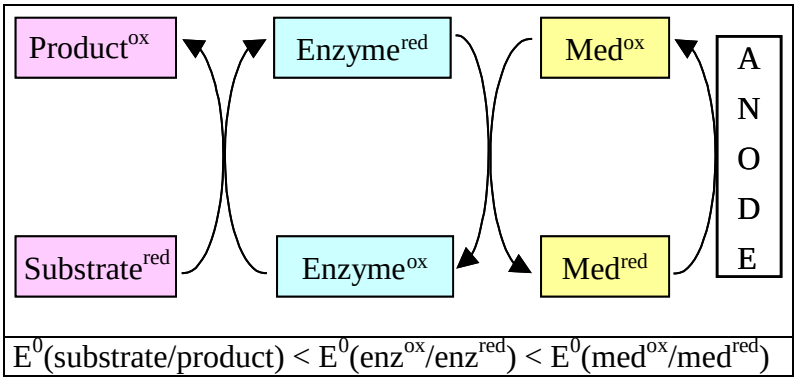

Fig. 3. Schematic depicting the electron flow in an enzyme-catalyzed mediated electron transfer oxidation of substrate. The relative magnitudes of the standard reduction potentials of each element for efficient mediation are shown beneath the scheme.

In redox mediation, to have an effective electron exchange, the thermodynamic redox potentials of the enzyme and the mediator have to be accurately matched. For biocatalytic electrodes, efficient mediators must have redox potentials downhill from the redox potential of the enzyme: a 50 mV difference is proposed to be optimal [1, 18]. The tuning of these potentials is a compromise between the need to have a high cell voltage and a high catalytic current. Furthermore, an obvious requirement is that the mediator must be stable in the reduced and oxidized states. Finally, for operation of a membraneless miniaturized biocatalytic fuel cell, the mediators for both the anode and cathode must be immobilized to prevent power dissipation by solution redox reactions between them.

12.4. Biocatalytic Cathodes

12.4.1. Enzymes and Substrates

In this section we review research on biocatalytic cathodes for oxidant reduction. The biocatalytic reduction of oxidants has only recently attracted renewed attention, with most research on biocatalytic fuels cells previously devoted to biocatalytic oxidation of fuels. However, in order to construct a biocatalytic fuel cell, it is essential to design a functional cathode for the reduction of the oxidant that is coupled to the anode and allows the

electrically balanced current flow. Conventional platinum metal cathode catalysts used in fuel cells for reduction of oxygen are usually not compatible with oxidation of biocatalytic fuels since they can be poisoned and passivated by components in the electrolyte. In addition, in the absence of a membrane assembly in miniaturized membraneless fuel cells, oxidation of the fuel can occur at the cathode catalyst [1-3]. Biocatalytic processes at the cathode offer the advantages of selectivity for the oxidant over fuel, allowing removal of the membrane assembly, and the possibility of decreasing poisoning and passivation, over traditional fuel cell catalytic processes. Inhibition and modulation of the biocatalytic processes remains however a major, unresolved, problem for technological advances in the adoption of prototype biocatalytic cathodes on an industrial scale.

We focus here on the use of oxygenases, particularly the "blue" copper oxygenases, such as laccase and bilirubin oxidase, that can biocatalytically reduce oxygen directly to water at relatively high reduction potentials under mild conditions. First, however, we will briefly consider reports on the use of hydrogen peroxide as an oxidant in biocatalytic fuel cells.

12.4.2. Peroxidases

The use of hydrogen peroxide as an oxidant is not compatible with operation of a biocatalytic fuel cell *in vivo*, because of low levels of peroxide available, and the toxicity associated with this reactive oxygen species. In addition peroxide reduction cannot be used in a membraneless system as it could well be oxidized at the anode. Nevertheless, some elegant approaches to biocatalytic fuel cell electrode configuration have been demonstrated using peroxidases as the biocatalyst and will be briefly reviewed here.

Peroxide is a strong oxidant, with a standard reduction potential of +1.78 V vs NHE, and is thus a good candidate for an oxidant [2b]. The direct reduction of peroxide at electrodes, however, has a high overpotential, thus necessitating the use of catalysts. A recent interesting development for the design of peroxide reducing cathodes is the use of ferrocene-mediated peroxide reduction by the enzyme horseradish peroxidase at electrodes prepared by spray-painting of graphite, enzyme, mediator and binder onto a polymeric support [19]. These electrodes demonstrated peroxide reduction occurring close to the ferrocene/ferricenium redox potential of ~ +0.25 V vs SCE (~ +0.50 V vs NHE). Willner and co-authors have developed an impressive protocol for the tethering and immobilization of microperoxidase-11 at gold electrodes, to yield electrodes that reduce peroxide by direct electron transfer to the microperoxidase [15,20,21]. Microperoxidases are produced via proteolytic digestion of cytochrome *c* (Cyt *c*) to yield a heme-bound peptide of six, eight, nine or eleven amino acids. Microperoxidase-11 thus consists of 11 amino acids and a covalently linked heme site. Microperoxidase-11 was covalently linked via carbodiimide coupling chemistry of carboxylic acid functions of the microperoxidase, to the terminal amine group of a self-assembled monolayer of cystamine on a gold electrode, yielding electrodes with redox potentials for microperoxidase-11 heme of ~ ─0.4 V vs SCE [20]. There is some doubt about whether a single monolayer of microperoxidase-11 forms using this coupling approach, or if multi-layers are formed, based upon examination of the rate of heterogeneous electron transfer to the microperoxidase-11 using this and other immobilization approaches [22]. The microperoxidase-11 modified electrodes were capable of biocatalytic reduction of peroxide at potentials as positive as +0.3 V vs SCE,

with the reason for this potential shift postulated to be a result of the formation of an Fe(IV) intermediate species in the presence of peroxide [20,23].

Recently, direct electron transfer to microperoxidases adsorbed on carbon nanotube-modified platinum electrodes has been observed [24]. The redox potential for this direct electron transfer is ~ ─0.4 V vs SCE, the same as that for the microperoxidase-11 on the cystamine-modified gold. However, curiously, biocatalytic reduction of peroxide proceeds at this redox potential, ─0.4 V vs SCE, at the carbon nanotube-modified electrodes, and not shifted positively, as was reported for the cystamine-modified gold [20].

Conversion of a peroxide reducing cathode into a cathode that reduces dissolved oxygen is also possible, as recently demonstrated by Ramanavicius et al. [25]. In this study, microperoxidase-8 was co-immobilized with glucose oxidase to provide a cathode that couples glucose oxidation, producing peroxide from the oxygen co-substrate, with peroxide reduction by the microperoxidase, and subsequent direct electron transfer from the electrode to the microperoxidase. Whilst this is an elegant demonstration of a novel combination of biocatalyst to provide high potential (~ +0.15 V vs SCE) reduction of oxygen, the fact that glucose is depleted, as it effectively acts as a co-substrate, would mitigate against adoption of this approach for an implantable biocatalytic fuel cell using glucose as a fuel.

12.4.3. Oxygenases

The theoretical thermodynamic reduction potential for oxygen is +1.23 V vs NHE at pH 0, or +0.82 V vs NHE at pH 7, and it is thus, like peroxide, a strong oxidant [1-3]. The reduction of oxygen at electrodes is, again like peroxide, hampered by large overpotentials, with direct electrochemical reduction occurring only at ~ ─0.1 V vs NHE at gold and carbon electrodes at neutral pH. Catalysts, such as platinum, are therefore used to decrease this overpotential in fuel cell cathodes. As stated previously, however, the use of expensive, and non-selective, platinum catalysts is not compatible with operation of a putative miniaturized membraneless fuel cell *in vivo*. An additional disadvantage of oxygen reduction at platinum catalysts is that it occurs, at neutral pH, via a two-electron reduction, to produce peroxide, a toxic reactive oxygen species *in vivo*.

Catalytic reduction of oxygen directly to water, whilst not as yet possible with traditional catalyst technology at neutral pH, is achieved with some biocatalysts, particularly by enzymes with multi-copper active sites such as the laccases, ceruloplasmins, ascorbate oxidase and bilirubin oxidases. The first report on the use of a biocatalyst in the cathode of a fuel cell for reduction of oxygen was by Palmore and Kim [26], who investigated the reduction of oxygen to water by a solution-phase laccase from *Pyricularia oryzae* using 2,2'-azinobis(3-ethylbenzothiazoline-6-sulfonate) (ABTS) as a diffusional mediator.

The laccases, classed as polyphenol oxidases, catalyze the oxidation of diphenols, polyamines, as well as some inorganic ions, coupled to the four-electron reduction of oxygen to water: see Fig. 4 for the proposed catalytic cycle. Due to this broad specificity, and the recognition that this specificity can be extended by the use of redox mediators [27], laccases show promise in a range of applications [28], from biosensors[29-32], biobleaching [27,33-35] or biodegradation [36], to biocatalytic fuel cells [1-3,18,26,37-42].

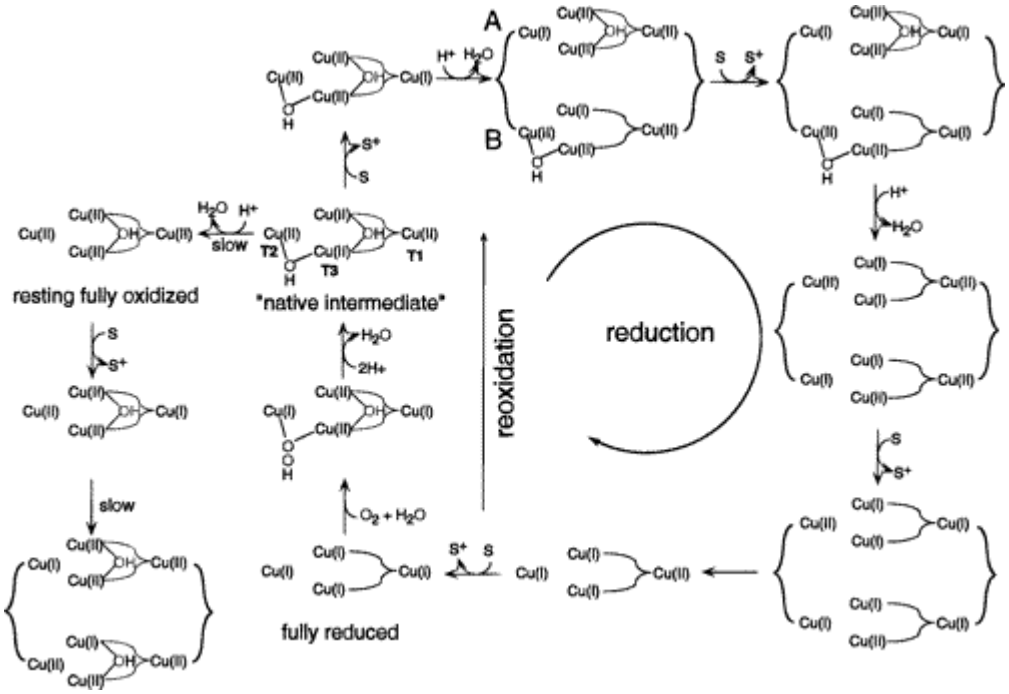

Fig. 4. Proposed catalytic cycle for laccase, where S represents substrate (from [44] with permission from the American Chemical Society).

Laccase was first isolated by Yoshida in 1883 [43] from tree lacquer of *Rhus vernicifera*. Laccases can thus be classified according to their source: plant, fungal, or, more recently, bacterial or insect [44]. The laccase enzyme active site contains four copper ions classified into three types based upon their geometry and co-ordinating ligands, denoted type 1 (T1), type 2 (T2), and type 3 (T3) [44]. The T2 and T3 coppers form a tri-nuclear cluster for reduction of oxygen, whereas successive one-electron oxidation of the substrates occur at the so-called "blue" T1 site, approximately 1.3 nm distal to the T2/T3 cluster. The key characteristic of the "blue" multi-copper oxygenases is the standard reduction potential of the T1 site. The catalytic efficiency of the laccase reaction with its substrate has been shown to depend on the thermodynamic driving force for electron transfer: the potential difference between substrate and T1 copper site [34,44-48]. Laccases possessing T1 sites of relatively high reduction potentials can drive oxidation of otherwise recalcitrant organic or biopolymeric substrates, finding application in bioremediation and dye and pulp bleaching. In addition, the oxidation of substrates coupled to intra-molecular electron transfer to the T2/T3 cluster can result in the reduction of oxygen at relatively high potentials. The reduction potential of the T1 site can be determined by redox titrimetry [44-49].

The copper-containing redox enzymes have also been shown to transfer electrons directly with electrode materials, allowing determination of the reduction potentials of the active site using voltammetry, and possible correlation with structure and activity. Direct electron transfer to a laccase was first reported by Yaropolov's group at carbon electrodes [50]. Subsequent studies [8,9,51,52] have investigated direct electron transfer to the copper active sites of the multi-copper oxidases as a means to classify the oxidases. The laccases can thus be classified, as suggested recently by Shleev et al. [9,10], into three separate

groups, based upon the reduction potential of the T1 copper site. The plant laccases have a low T1 potential of ~ +0.43 V vs NHE, whilst fungal laccases possess T1 sites of, either middle potential of +0.47 to +0.71 V vs NHE, or high potential of ~ +0.78 V vs NHE.

Whilst direct electron transfer to laccases may help elucidate the mechanism of action of these enzymes it is unlikely that this process will supply sufficient power for a viable implantable biocatalytic fuel cell, because of difficulties associated with the correct orientation of the laccase and the 2-dimensional nature of the biocatalytic layer on the surface. However, a recent attempt to immobilize laccase in a carbon dispersion, to provide electrodes with correctly oriented laccase for direct electron transfer, and a higher density of electrode material shows promise [53].

Mediated reduction of oxygen by laccase, particularly from fungal sources with high T1 potentials, as demonstrated by Palmore and Kim [26], does show great promise for the development of biocatalytic fuel cell cathodes. Immobilization of both mediator and laccase provides a biocatalytic cathode for oxygen reduction that may be used in a miniaturized membraneless biocatalytic fuel cell. Trudeau et al. [30] were the first to report on oxygen reduction by films of immobilized mediator and laccase, formed by cross-linking laccase to an osmium-based redox polymer film on carbon electrodes. The redox polymer, structure shown in Fig. 5, was prepared by substitution of one of the chloride ligands of an Os(2,2'-bipyridine)$_2$Cl$_2$ complex, with every tenth imidazole monomeric unit of the polyvinylimidazole polymer backbone.

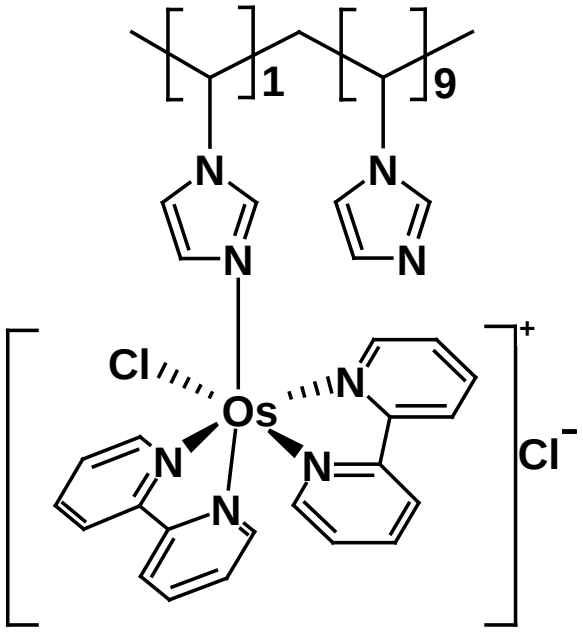

Fig. 5. Structure of the osmium redox polymer, formed by co-ordination of a [Os(2,2'-bipyridine)$_2$Cl]$^+$ complex to polyvinylimidazole in a usually 1:9 ratio.

Co-immobilization of this redox polymer with a fungal laccase from *Trametes versicolor*, possessing a T1 copper site reduction potential of ~ +0.57 V vs Ag/AgCl (~ +0.77 vs NHE), was achieved using a diepoxide cross-linker, in an approach pioneered by the Heller group [54]. Although the laccase biocatalytic electrode was developed for the reagentless detection of modulators of enzyme activity, steady-state current densities of

greater the 125 μAcm^{-2} were achieved at potentials of ~ +0.15 V vs Ag/AgCl in oxygen sparged acetate buffered solutions, pH 4.5, as shown in the cyclic voltammograms in Fig. 6 [55]. Subsequent to this report, this group and others have investigated mediated laccase catalyzed reduction of oxygen in films of redox polymers on electrode surfaces for application as biocatalytic cathodes. For example, substitution of the chloride ligand of a [Os(4,4'-dimethyl, 2,2'-bipyridine)(2,2':6',2''-terpyridine)Cl]$^{+}$ complex with imidazole units of PVI yields a redox polymer that may be co-immobilized with laccase from *Coriolus hirsutus* on carbon cloth fibre. The resulting biocatalytic oxygen cathodes operate at mAcm^{-2} current densities at a potential of +0.7 V vs NHE in pH 5 buffer, 37°C, when rotated at 4000 rpm [37].

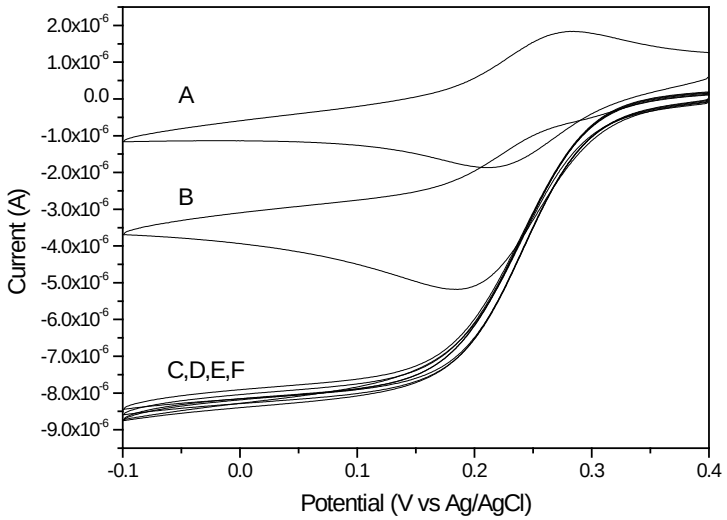

Fig. 6. Cyclic voltammograms at a laccase biosensor in the absence (A) and presence (B) of O_2. Sparging of O_2 through the electrolyte between scans (2 minutes) yields reproducible and increased catalytic reduction currents (C-F) compared to ambient O_2 levels. Scan rate 10 mVs^{-1} in 0.05 M acetate buffer of pH 4.5. (From reference [55] with permission from Wiley.)

Further refinement of this cathode is also possible, by judicious choice of biocatalyst. The high potential fungal laccases are reportedly sensitive to chloride inhibition and have optimal acidic pH maxima, for example, seemingly precluding their use in physiological solutions. Co-immobilization of the redox polymer described above with a laccase from *Pleurotus ostreatus*, which has been reported to retain a high level of substrate oxidation activity at pH 7, yielded biocatalytic oxygen cathodes capable of operating at +0.62 V vs NHE in pH 7, 0.1 M NaCl solution at 37°C, with 6% of their pH 5, chloride-free, current density [40].

The chloride and pH sensitivity of the laccase catalyzed oxygen reduction has led some groups to focus on another class of "blue" copper enzymes, that are active under physiological conditions of pH and NaCl, the bilirubin oxidases. Bilirubin oxidase catalyzes the oxidation of bilirubin to biliverdin coupled to the four-electron reduction of oxygen to water. The catalytic site of BOD, like laccase, consists of a tri-nuclear T2/T3 oxygen-reducing copper site and a T1 substrate oxidizing copper site [44,45]. Unfortunately, the reduction potential of the T1 site of the bilirubin oxidases is of the

medium potential classification of ~ +0.3 V vs Ag/AgCl [9,10,45]. The first report on a BOD-based biocatalytic oxygen cathode focused on homogeneous ABTS mediated reduction of oxygen at carbon felt electrodes using a BOD from *Myrothecium verrucaria* (*Mv*) in phosphate buffer, pH 7.0 [56]. Subsequent optimization of the BOD cathode focused on immobilization of both mediator and enzyme, and matching of mediator redox potential to that of the enzyme. The Ikeda group have achieved current densities of 17 $mAcm^{-2}$ at +0.25 V vs Ag/AgCl for mediated oxygen reduction by electrostatically entrapping *Mv*BOD with $[W(CN)_8]^{3-/4-}$ in poly(L-lysine) at carbon felt electrodes rotated at 4000 rpm [57]. The Heller group have co-immobilized *Mv*BOD and a redox polymer prepared by substitution of one of the chloride ligands of a Os(4,4'-dichloro-2,2'-bipyridine)$_2$Cl$_2$ complex with imidazole units of a copolymer of poly(vinylimidazole) and polyacrylamide on carbon cloth fibers to yield biocatalytic oxygen cathodes that provide current densities of 0.7 $mAcm^{-2}$ at a potential of +0.3 V vs Ag/AgCl in non-stirred phosphate buffered saline at 37 °C [58]. Further improvements in the BOD cathode were obtained by replacement of the *Mv*BOD by a BOD from *Trachyderma tsunodae*, which is claimed to have a T1 redox potential of +0.44 V vs Ag/AgCl. Current densities of 6.25 $mAcm^{-2}$ at potentials of +0.3 V vs Ag/AgCl were obtained at carbon cloth electrodes rotated at 4000 rpm in oxygenated phosphate buffered saline at 37 °C [59]. Purification of the BOD yielded biocatalytic films that provided higher current densities of 9.5 $mAcm^{-2}$ under these conditions [60]. More recently, direct electron transfer "type" reactions of the *Mv*BOD enzyme immobilized in poly(L-lysine) layers at carbon electrodes containing a high density of crystal edges have been reported [61]. Using this approach, from the cyclic voltammograms (CV's) in Fig. 7, steady-state current densities of 0.85 $mAcm^{-2}$ for oxygen reduction at potentials of ~ +0.2 V vs Ag/AgCl in oxygen saturated phosphate buffer at pH 7.0 with rotation at 1400 rpm can be estimated.

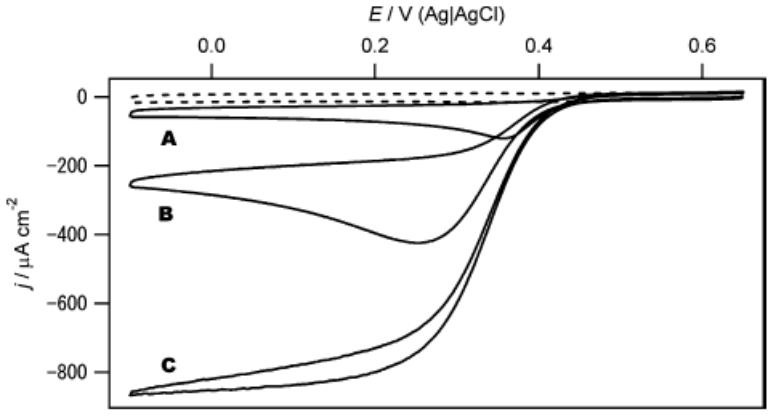

Fig. 7. Cyclic voltammograms recorded at carbon electrodes containing *Mv*BOD enzyme immobilized in poly(L-lysine) layers. (A) Air saturated in quiescent solution. (B) O_2 saturated conditions without stirring. (C) O_2 saturated conditions with stirring at 1400 rpm. Dashed line represents the CV recorded under Argon. (From [61] with permission from Elsevier.)

12.5. Biocatalytic Anodes

12.5.1. Enzymes and Substrates

In this section, the enzymes, and associated substrates, used as biocatalysts in anodes are presented. For the development of biocatalytic anodes, there is a wide range of fuels available for use as substrates, such as alcohols, lactate, hydrogen, fructose, sucrose, all of which can be oxidized by biocatalysts. The fuel that is the most widely considered, however, in the context of an implantable biocatalytic fuel cell is glucose. We shall focus our attention on this fuel, but will mention briefly research on the use of some other fuels in biocatalytic anodes.

12.5.2. Glucose Oxidase

Glucose oxidase (GOx) is an FAD (Flavin Adenine Dinucleotide, see Fig. 8) enzyme which very specifically oxidises β-D-glucose, reducing dioxygen to hydrogen peroxide in the process. Glucose is an attractive substrate, for future implantable devices, because of its relatively high concentration in blood, of around 9 mM, and also because GOx is an extremely stable enzyme with high substrate specificity.

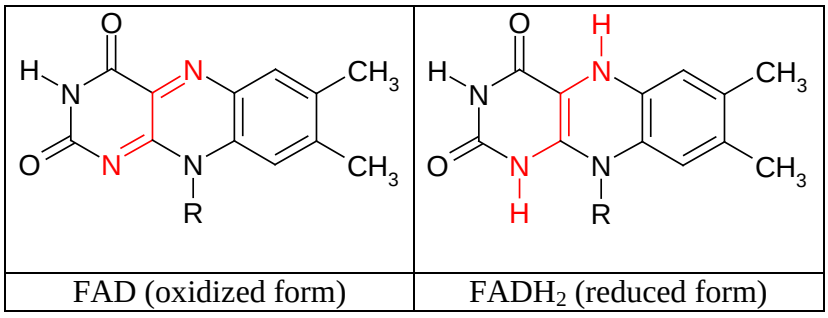

FAD (oxidized form)	$FADH_2$ (reduced form)

Fig. 8. Structure of the $FAD/FADH_2$ active site of glucose oxidase

As referred to previously, if the active site of a biocatalyst is close enough to the electrode surface, direct electron transfer to/from an electrode can result. It has been shown in recent years that direct electron transfer from the GOx active site is possible using appropriate electrode preparation procedures. These preparation procedures usually aim to provide nano-structured features on the electrode surface that can penetrate sufficiently the GOx active site to allow for direct electron transfer. The direct electron transfer occurs between the $FAD/FADH_2$ active site of the GOx and the electrode surface, at redox potentials close to the −0.41 V vs SCE reduction potential of FAD [62] at neutral pH. Examples of direct electron transfer to GOx have been reported for GOx adsorbed or attached to carbon paste [63], carbon nanotube [64-66] and colloidal gold nanoparticles [67,68] modified electrodes. However, in these cases the electrode replaces the glucose substrate, thus resulting in the biocatalytic reduction of oxygen to hydrogen peroxide, in the presence of oxygen.

$$GOD(FAD) + 2e^- + 2H^+ \rightleftharpoons GOD(FADH_2) \quad (1)$$

$$GOD(FADH_2) + O_2 \rightarrow GOD(FAD) + H_2O_2 \quad (2)$$

In the presence of glucose and oxygen the bioelectrocatalytic reduction of oxygen is diminished due to competition for the FAD active site between glucose and the electrode surface. A method for the determination of glucose levels, based on this decrease in reduction current in the presence of glucose, has been proposed [67]. In the presence of anaerobic glucose solutions, only the redox process for $FAD/FADH_2$ is observed, with no biocatalytic oxidation of glucose. In conclusion, the direct electron transfer to GOx at nano-structured electrode surfaces yields biocatalytic oxygen reduction currents. GOx direct electron transfer processes cannot therefore be usefully used as yet to develop an anode for biocatalytic fuel cells.

Since the first report on the ferrocene mediated oxidation of glucose by GOx [69], extensive solution-phase studies have been undertaken in an attempt to elucidate the factors controlling the mediator-enzyme interaction. Although the use of solution-phase mediators is not compatible with a membraneless biocatalytic fuel cell, such studies can help elucidate the relationship between enzyme structure, mediator size, structure and mobility, and mediation thermodynamics and kinetics. For example, comprehensive studies on ferrocene and its derivatives [70] and polypyridyl complexes of ruthenium and osmium [71,72] as mediators of GOx have been undertaken. Ferrocenes have come to the fore as mediators to GOx, surpassing many others, because of factors such as their mediation efficiency, stability in the reduced form, pH independent redox potentials, ease of synthesis and substitutional versatility. Ferrocenes are also of sufficiently small size to diffuse easily to the active site of GOx. However, solution phase mediation can only be used if the future biocatalytic fuel cell is to be used as a non-implantable device, because of the need for a membrane and casing.

The mediator and enzyme can be immobilized by adsorption onto electrodes, linkage functionalized to the electrode surface or integration into a polymer layer. The immobilization of biocatalyst and mediator provides the possibility for membrane-less biocatalytic fuel cells, because of effective separation of the anode and cathode reagents. The easiest way to immobilize mediators is through adsorption onto electrode surfaces. Cass et al. [69] deposited solutions of ferrocene derivatives onto pyrolytic graphite electrodes and allowed them to air-dry. In this approach, the solubility of ferrocenes in aqueous solution must be low to aid entrapment within the electrode. Covalent attachment of GOx (through carbodiimide activation) to the electrode and covering with polycarbonate membranes provided biocatalytic surfaces for mediated oxidation of glucose. All the ferrocene derivatives investigated act as rapid oxidants for the enzyme glucose oxidase [69,70].

Increased micro and nano-scopic surface areas can lead to improved signal output for mediated biocatalytic electrodes. For example, Liu et al. [73] used porous carbon as a matrix to load glucose oxidase to provide an anode in a biocatalytic fuel cell. Not surprisingly, given the increased loading of enzyme, this biocatalytic anode displayed higher oxidation currents than that observed for GOx on a glassy carbon electrode in the presence of glucose and solution phase ferrocene monocarboxylic acid as a mediator. The

formal potential of the mediator of +0.34 V vs Ag/AgCl is, however, remote from the $FAD/FADH_2$ reduction potential and further refinement of this system is focused on selecting more appropriate mediators and the co-immobilization of the mediator with enzyme.

Co-immobilization of mediator and enzyme may be achieved using a novel reconstitution approach. For example, Katz et al. [15] have developed a biocatalytic anode functionalized by a surface reconstitution of apo-GOx onto FAD that was previously coupled to a pyrrolo-quinoline quinine (PQQ) relay conjugated to a self-assembled monolayer of cysteamine on gold. The CV study of this assembly in the presence of glucose yields an electrocatalytic current for glucose oxidation commencing at −0.12 V vs. SCE at pH 7. The chronoamperometric output from this assembly can achieve current densities of 300 $mAcm^{-2}$ at +0.2 V vs SCE in 80 mM of glucose [2b]. Further modification, to what the authors term the electrical contacting of the enzyme, involved the use of alternate conjugation strategies [74], and of nano-structured surfaces [75,76]. Xiao *et al.* [76] have reconstituted apo-GOX onto FAD-functionalized gold nanoparticles that are then tethered via a dithiol spacer to a bulk gold electrode. This gold nanoparticle assembly is an efficient relay of electrons between the FAD active site and the bulk electrode. Unfortunately, the biocatalytic oxidation of glucose using this assembly only commences at potentials greater than +0.4 V vs SCE, with the overpotential proposed to result from a tunnelling barrier introduced by the dithiol spacer.

An alternative strategy for co-immobilization of mediator and GOx is based on adsorption of enzyme, cross-linked, as was described for the laccase-based biocatalytic cathodes [30,37-42], to an osmium-based redox polymer film, on carbon electrodes [1-3,54]. In the case of these redox-polymer mediators a key parameter to take into account is usually the polymer/enzyme ratio [30,77,78]. An excessive enzyme weight fraction can decrease the current density because the enzyme is an electronic insulator. When the weight fraction of redox polymer is excessive, the flux of electrons is reduced because of the smaller number of enzyme molecules. The initial studies on these redox polymer GOx films for mediated oxidation of glucose focused on co-immobilization with the OsPVI polymer shown in Fig. 4 on carbon electrodes [42,54]. Refinement of the redox potential of the polymer was achieved by replacing the 2,2'-bipyridine ligands of osmium with, initially, 4,4-dimethyl- 2,2'-bipyridine, resulting in biocatalytic oxidation of glucose at ~ +0.1 V vs Ag/AgCl compared to +0.25 V vs Ag/AgCl [79]. Replacement of this ligand with 4,4'-dimethoxy-2,2'-bipyridine, subsequent to a report by Zakeerudin *et al.* [71] on increased electron transfer rates from GOx to osmium complexed to such ligands, yielded a redox polymer with a redox potential of −0.07 V vs Ag/AgCl [54]. Finally, further refinement of the redox polymer is possible by replacement of the 2,2'-bipyridine ligands of osmium with 4,4'-diamino-2,2'-bipyridine, to yield a redox potential of ~ −0.15 V vs Ag/AgCl [77]. A current density of ~ 65 $\mu A/cm^2$ was observed for oxidation of 10 mM of glucose in room temperature pH 7.4 phosphate buffered saline solution at films of GOx co-immobilized with the latter redox polymer on graphite electrodes. This output may be improved upon by the use of electrode surfaces of higher micro- and nano-scopic areas. For example a current density of ~ 150 $\mu A/cm^2$ was observed for similar films immobilized on a 7 μm diameter carbon fibre electrode, in solutions containing 15 mM glucose, pH 7.4 in phosphate buffered saline at 37 °C [77,80].

A significant limiting factor to current density output in these redox polymer films is the ease of physical displacement of the redox centre in the polymer film to allow intimate contact, and electron transfer, between the redox complex and the biocatalyst [81]. To address the mobility of the redox complex sites in the redox polymer, represented by an apparent diffusion co-efficient *D*, Mao et al. [82] have grafted a 13-atom-long flexible spacer between a poly(vinylpyridine) polymer backbone and an alkyl functional group of a $[Os(N,N'\text{-dialkylated-}2,2'\text{-biimidazole})_3]^{2+/3+}$ redox centre. This strategy allows both improved electron transfer between GOx-$FADH_2$ centres and the redox polymer, and charge transport within the redox polymer. Carbon fibres coated with cross-linked films of GOx and this polymer have a redox potential of −0.19 V vs. Ag/AgCl, and provide a current density of 1.15 $mAcm^{-2}$ in solutions containing 15 mM glucose, pH 7.4 in phosphate buffered saline at 37 °C. A further improvement in current density, to yield 1.5 $mAcm^{-2}$ at a potential of −0.1 V vs Ag/AgCl, is obtained when the ratio of osmium complex to polymer monomeric unit is optimised [83].

It should be noted that biocatalytic fuel cell anodes based on the GOx enzyme face a significant problem: O_2 is the natural electron acceptor of GOx. GOx therefore catalyzes the oxidation of glucose to gluconolactone, producing also hydrogen peroxide when dioxygen is the electron acceptor. The mediators described previously attempt to compete with the oxygen reduction in order to avoid oxygen depletion, because it is required for the cathode, and production of peroxide, a highly toxic product. It may, therefore, be interesting to focus on enzymes which oxidize fuels yet don't produce hydrogen peroxide, such as dehydrogenases.

12.5.3. Dehydrogenases

Dehydrogenases, which represent a majority of redox enzymes are mostly NAD (Nicotinamide Adenine Dinucleotide see Fig. 9) dependent. This cofactor is not directly bound to the enzyme but its presence in the medium is necessary because it acts as a carrier of two electrons and one proton, and it activates the biocatalytic function of the enzyme.

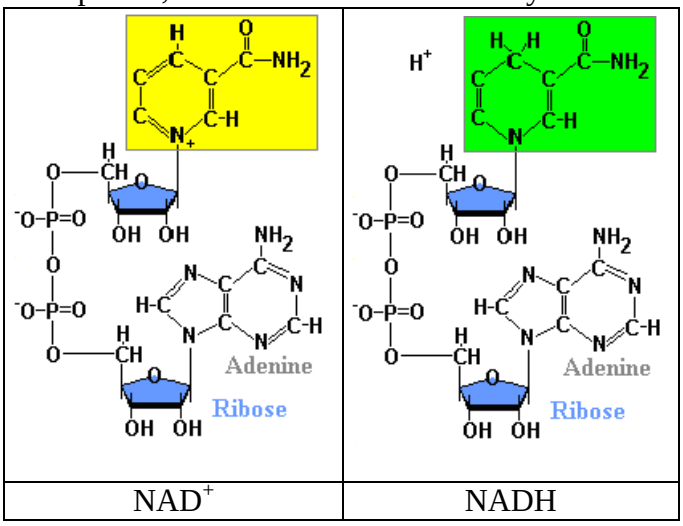

Fig. 9. Structure of the NAD^+/NADH co-factor

The thermodynamic redox potential of NAD^+/NADH is –0.56 V vs. SCE at neutral pH. The NADH co-factor itself is not a useful redox mediator because of the high overpotential and lack of electrochemical reversibility for the NADH/NAD^+ redox process, and the interfering adsorption of the cofactor at electrode surfaces.

As dehydrogenases (DH) are widely distributed enzymes, a number of studies have been carried out with these biocatalysts. For example, Willner et al. [20] have used a PQQ-monolayer functionalized gold electrode for the catalytic oxidation of NADH in the presence of Ca^{2+}. In this scheme, the pyrrolo-quinoline quinine co-factor, PQQ, was covalently linked, as before for the GOx system [15,20,21], to the Au-electrode, and was capable of oxidizing NADH at ~ –0.15 V vs. SCE at pH 8.0. A theoretical current density of 185 $\mu A/cm^2$ is estimated for this monolayer-modified system. This method is attractive as it may be applied to oxidative reactions of the dehydrogenases for which NAD is the cofactor.

Glucose dehydrogenase (GDH) is a class of enzyme that is gaining increased attention as a catalyst for the oxidation of glucose in biosensing and biocatalytic fuel cell applications. GDH is either a NAD^+- or PQQ-dependent enzyme. The pyrrolo-quinoline quinine (PQQ) co-factor (prosthetic group) has a thermodynamic redox potential of ─0.125V vs SCE at pH 7 [20], which is less negative than that for the NAD^+/NADH couple. In addition, the application of the PQQ-dependent GDH to biocatalytic fuel cells may be limited because of its relative instability with respect to GOx [84]. Nevertheless, the application of electrodes modified with the PQQ-dependent GDH as glucose sensors and biocatalytic anodes has been explored owing to its oxygen insensitivity, the fact that the co-factor is bound to the enzyme, unlike the NAD^+-dependent GDH, and the high catalytic efficiency of this PQQ-dependent GDH [84-87]..

For example, Ye et al. [85] have used carbon electrodes coated with cross-linked films of soluble PQQ-dependent GDH, from *Acinetobacter calcoaceticus*, and an osmium redox polymer to achieve glucose oxidation current densities of 1.8 $mAcm^{-2}$ at +0.4 V vs SCE in solutions containing glucose concentrations above 40 mM. Tsujimura et al. [87] have recently utilized this approach to devise a biocatalytic fuel cell anode for glucose. Zayats et al. [74], in an approach similar to that devised for the apo-GOx system [15,20,21], have reconstituted PQQ-dependent apo-GDH on PQQ-functionalized gold nanoparticles assembled onto a gold surface. Unfortunately, whilst the onset of bioelectrocatalytic oxidation of glucose is close to the redox potential of the PQQ, ─0.125V vs SCE at pH 7, appreciable glucose oxidation currents are only observed at an overpotential of approximately 0.35 V vs the PQQ redox potential, at +0.2 V, precluding its use as a biocatalytic anode for glucose oxidation. This overpotential is similar to that observed for re-constituted apo-GOx on gold nanoparticles (*vide supra*) and is again attributed to a tunnelling barrier introduced by the dithiol spacer.

Yuhashi et al. [84] have described a biocatalytic fuel cell anode for glucose based on PQQ-dependent GDH carbon paste electrodes. The enzyme mixed with carbon paste is lyophilized and then packed into the end of a carbon electrode and treated with glutaraldehyde for immobilization. The research was extended to investigate improving the stability of the GDH using a Ser415Cys mutant GDH, previously developed for biosensor applications [88]. For the wild-type GDH, after 24 hours of operation only 40% of the

initial catalytic response remained. Meanwhile, the Ser415Cys mutant GDH, showed improved stability, with 80% of the initial response remaining after the same period [84].

The use of the NAD^+-dependent GDH as a glucose biocatalytic anode has been investigated recently by Sato et al [89]. This research focused on evaluating the use of glassy carbon electrodes coated with diaphorase/GDH and a polymeric vitamin K_3-based mediator with a redox potential of −0.25 V vs Ag/AgCl at pH 7, as a glucose oxidising anode. Vitamin K_3 had previously been identified as a promising mediator of the diaphorase oxidation of NADH to NAD^+ [90]. The anode operation is thus based on vitamin K_3 mediation of diaphorase oxidation of NADH to NAD^+ and GDH oxidation of glucose coupled to NAD^+ reduction.

Palmore et al. [91] have reported on a graphite plate biocatalytic anode that uses solution phase dehydrogenases to catalyse the successive oxidation of methanol to CO_2. Whilst this anode is not useful in the context of implantable fuel cells, it is of interest because methanol is an attractive anodic fuel due to its availability and ease of transport and storage. The oxidation of one equivalent of methanol requires the reduction of three equivalents of NAD^+ to NADH. As the NADH cofactor itself is not a useful redox mediator, a benzylviologen/diaphorase redox cycle, with a redox potential of −0.55 V vs SCE at pH 7, was used to regenerate NAD^+ for use by the dehydrogenases, as depicted in Fig. 10.

Simon et al. [92] investigated a biocatalytic anode based on lactate oxidation by lactate dehydrogenase (LDH). The anodic current is generated by the oxidation of NADH (produced by NAD^+ and substrate) whilst LDH catalyzes the electro-oxidation of lactate into pyruvate. As previously mentioned, the oxidation of NADH at bare electrodes requires a large overpotential, so these authors used poly(aniline) films doped with polyanions to catalyze NADH oxidation. Subsequent research by this group focused on targeting mutants of LDH that are amenable to immobilization on the polyaniline surface [93].

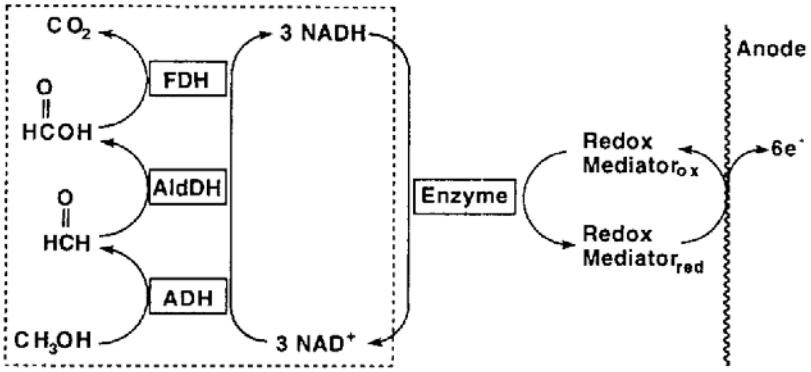

Fig. 10. Oxidation of methanol to CO_2, catalyzed by NAD^+-dependent alcohol (ADH), aldehyde (AldDH) and Formate (FDH) dehydrogenase, with regeneration of NAD^+ via redox mediation to diaphorase. (From reference [91] with permission from Elsevier.)

12.6. Biocatalytic Fuel Cells

12.6.1. Physiological Conditions

In this section, recent progress on assembled biocatalytic fuel cells is reviewed. One long term goal of biocatalytic fuel cell research is the development of a low-powering device implanted in the human body and extracting electrical energy through the oxidation of a biocatalytic fuel (eg. glucose) and reduction of a bio-available oxidant (e.g. O_2). Therefore it is important to keep in mind the basic physiological conditions such as, among others, concentration of substrates or inhibitors, fluid pH, temperature and velocity, that will eventually become the immediate working environment of the implanted biocatalytic fuel cell. Although the list focuses on blood parameters, it is not exhaustive and other physiological tissues may be considered as well for an eventual implantation.

The dioxygen partial pressure in blood vessels is about 95 mmHg in arteries and 40 mmHg in veins which corresponds to a concentration of respectively ~ 2.14×10^{-4} M and 5.4×10^{-5} M in free dioxygen. The concentration of glucose in blood vessels is *ca*. 9 mM in healthy adults. Chloride is the anion present in the highest concentration in physiological media with chloride concentration in blood about 136-145 mM. It is an important plasmolyte to take into account as it can be an inhibitor of some enzymes, for instance via binding to copper sites in some oxidases. Other anions present in appreciable concentration are bicarbonate (~10 mM) phosphate (~ 0.6 mM) and sulfate (~ 0.2 mM). Sodium is the main cation in blood (132 to 144 mM) followed by potassium 4 mM, calcium, 2 mM and magnesium, 1 mM. Other elements such as, aluminium, copper, fluorine, iron and zinc, are present in low concentration (~ 5 to 30 μM), whilst manganese, lead, tin, bromine and iodine are present in very low concentration (~ 0.1 to 5 μM). Blood is a buffered solution with a pH of 7.4. Other body fluids are also close to neutral pH, like, for example, saliva at the pH of 7.2. A notable exception is acidic gastric juices (pH 2). The human body is also thermostated at 37 °C, a peculiarity common to all mammals where constant body temperature lies in the range 34 to 40 °C depending on the species. The velocity of blood in blood vessels is of the order of 1 to 10 cm/s. Other body fluids may be considered as well, for instance the pH of tears is ca. 7.5 and contains, not surprisingly, low levels of glucose (50-500 μM).

12.6.2. Assembled Glucose-oxygen Biocatalytic Fuel Cells

Many assembled glucose-O_2 biocatalytic fuel cells have been reported in recent years. This section aims at giving an overview of the methods that have been used to build these biocatalytic fuel cells and of the performances obtained by these devices depending on their different designs.

Katz et al. [17] reported on a biocatalytic fuel cell based on the surface reconstitution of apo-GOx onto FAD that was previously coupled to a pyrrolo-quinoline quinine (PQQ) relay conjugated to a self-assembled monolayer of cysteamine on gold. The cathode consisted of a cross-linked affinity complex between cytochrome *c* (Cyt. *c*) and cytochrome *c* oxidase (COx) assembled on gold through a thiol modified Cyt. *c* promoter. The promoter is a maleimide monolayer that is specifically reacted with the cysteine102

residue of Cyt. *c* from *Saccharomyces cerevisae* ensuring proper alignment between the electrode surface and the heme site of the protein, and consequently electrical communication between the electrode and the protein. Electron transfer between the biocatalyst and the electrode was particularly efficient at the anode and thought not to be perturbed by molecular oxygen, the natural electron donor, nor by typical interfering species like ascorbic acid or uric acid. Comparatively, interfacial electron transfer was much less efficient at the cathode. The reduction of O_2 occured at 0 V vs SCE at the cathode whilst oxidation of glucose at the anode occured at the potential of PPQ (−0.12 V vs. SCE at pH 7). The maximum reported power for this cell was 4 μW at a load of 0.9 kΩ and an electromotive force of 50 mV (power density 5 μWcm^{-2}). The cell was studied for 48 hours in a flow system under constant glucose concentration (1 mM) under air and showed no sign of current or cell potential decrease.

A biocatalytic fuel cell reported by Tsujimura et al. [87] is based on polished glassy carbon electrodes modified by *Mv*BOD for the anode and PQQ-GDH from *Acenitobactor calcoaceticus* for the cathode. Redox mediation is effected by $[Os(2,2'\text{-bipyridine})_2Cl]^+$ conjugated to poly(4-vinylpyridine) quaternized with bromoethylamine (redox potential of 0.35 V vs. Ag/AgCl) for the cathode, while the anode contains $[Os(4,4'\text{-dimethyl-}2,2'\text{-bipyridine})_2Cl]^+$ conjugated to poly(vinylimidazole) (redox potential of +0.15 V vs. Ag/AgCl). The cell, assembled and studied in MOPS buffer, pH 7, containing 3 mM $CaCl_2$, yielded an open circuit voltage of 0.44 V (25 °C), with maximum current density of 430 μAcm^{-2} and maximum power density of 58 μWcm^{-2} at a cell potential of 0.19 V. The cathode was identified as limiting the cell performance, as a three times lower current density than the anode was obtained under the same conditions. The advantage of using the GDH enzyme at the anode rather than GOx, in addition to insensitivity to O_2, is that GDH is more tolerant to redox mediators of redox potential close to that of the enzyme. Indeed, the authors showed that despite a higher E^0 (–0.18 V for GDH and –0.35 V for GOx at pH 7) the bio-anode modified with GDH and the 0.15 V redox polymer yielded more than twice the current density than that modified with GOx and the same redox polymer. Finally GDH is less substrate selective than GOx. This is a drawback for glucose determination but may be an advantage for some fuel cell applications. The fuel cell stability was not reported but the need to stabilize the GDH enzyme was stressed.

Recently, Yuhashi et al. [84] attempted to address the GDH instability by using a mutated GDH (Ser415Cys). Their glucose-O_2 glucose dehydrogenase/bilirubin oxidase biocatalytic fuel cell was studied in a two compartment cell linked by a salt bridge and containing ABTS and phenazine methosulfonate (PMS) redox mediators in the cathode and anode compartment respectively. The electrodes were made by packing of a lyophilized mixture of the enzyme and carbon paste at the surface of a carbon electrode, followed by treatment by a 1% glutaradehyde solution. The anode was allowed to undergo holoformation in a solution containing $CaCl_2$ (1 mM) and PPQ (5 μM) before use. The open circuit voltage of the cell was 0.577 V (25 °C, pH 7). The maximum current density was 61.4 μAcm^{-2} under stirring (250 rpm) and the maximum power density was 17.6 μWcm^{-2} at a cell potential of 0.5 V with an external load of 200 kΩ. The half life of the cell was under a week, while that of the wild-type GDH was only two days. The eventual inactivation of the cell is ascribed to mediator instability. Sato et al. [89] used a NAD^+-dependent GDH anode that was coupled to a platinum cathode, not modified by any bio-

catalyst, in their fuel cell. Diaphorase from *Bacillus stearothermophilus*, was co-immobilized with polyallylamine functionalized with a derivative of Vitamin K_3 as the redox mediator to yield a NADH oxidation layer. A second layer of an electrostatic adduct between GDH and polylysine effected glucose oxidation. Crucial to the efficient electrical conduction between the Vitamin K_3 mediator and the electrode was the addition of carbon black in the diaphorase layer. Indeed the current density was two orders of magnitude higher in the presence of the conducting material. The "double-layer" design of the anode implies that the optimized diaphorase layer may be used with other NADH dependent enzymes such as alcohol dehydrogenase. The platinum cathode was coated with polydimethylsiloxane to yield an O_2-selective electrode. The assembled biocatalytic fuel cell was studied at 37 °C in air saturated phosphate buffer solution at pH 7 containing glucose (10 mM) and NADH (0.5 mM). The maximum power density was 14.5 μWcm^{-2} (40.3 μAcm^{-2} current density) at a potential of 0.36 V with an external load of 200 kΩ. The cell power dropped steadily for five days to 30% of its initial value and was then stable at about 4 μWcm^{-2} for more than two weeks. The use of a non-biocatalytic cathode is interesting in terms of electrode stability, whilst obvious bio-compatibility of vitamin K_3 is attractive for the prospect of an implantable device. However, the reduction product of oxygen at pH 7 is inevitably hydrogen peroxide.

Despite the known loss of activity of fungal laccase enzymes at neutral pH, and its reported inhibition by chloride, we were curious to investigate what cell performance could be reached with a *Trametes versicolor* laccase in a glucose-O_2 biocatalytic fuel cell working in pseudo-physiological conditions [18]. Our pseudo-physiological media was a pH 7.4 phosphate buffer containing 0.1 M sodium chloride and 10 mM glucose. The solution was thermostated under air at body temperature (37 °C). Graphite electrodes were modified by a mixture of enzyme, redox polymer and diepoxide crosslinker. The GOx-based anode redox polymer was $[Os(4,4'\text{-diamino-}2,2'\text{bipyridine})_2Cl]^+$ conjugated to polyvinylimidazole, of redox potential −0.11 V vs. Ag/AgCl. A $[Os(1,10\text{-phenanthroline})_2]^{2+}$ complex conjugated to two units of imidazole in a polyvinylimidazole polymer, of redox potential 0.49 V vs. Ag/AgCl, was used at the cathode. At pH 7.4 the maximum power density for the cell was 16 μWcm^{-2} at a cell voltage of 0.25 V. The fact that the cathode was limiting the device in this case is exemplified by the higher maximum power density of 40 μWcm^{-2} at pH 5.5, where laccase is much more active. Liu et al. [73] have exploited the pH dependence of laccase to build a biocatalytic fuel cell with a tunable power ouput. To increase power density porous carbon was chosen as the electrode material and GOx and laccase enzymes were entrapped in suspensions of carbon nanotube/chitosan and then cast on the porous carbon matrix. Solution redox mediators ferrocene monocarboxylic acid and ABTS were dissolved, respectively, in the anolyte and catholyte that were separated by a nafion membrane. The maximum power density dropped from 100 μWcm^{-2} at pH 4 to 2 $\mu W/cm^{-2}$ at pH 7.

The biocatalytic fuel cell prototypes presented have not as yet been refined in a rational manner. The situation is different for the cells designed by the Heller group, where an extensive literature is available. The publication of the first oxygen-glucose biocatalytic fuel cell from this group appeared in 2001 [38], after several years of refining each individual electrode [3]. One interesting aspect of their study is the miniaturization of the cell by the use of small carbon fibers (~3 cm long, 7 μm diameter and 0.44 mm^2 active

area) as the electrode material. The fibers were first rendered hydrophilic by plasma oxidation, and modified by a mixture of enzyme, an osmium-based redox polymer and a diepoxide crosslinker. The GOx anode was modified with [Os(4,4‘-dimethyl-2,2‘-bipyridine)$_2$Cl]$^+$ complex conjugated to a polyvinylimidazole *co*-acrylamide polymer, redox potential of +0.10 V vs. Ag/AgCl, while the laccase (*Coriolus hirsitus*) cathode had [Os(4,4‘-dimethyl-2,2‘-bipyridine)$_2$(2,2‘,6‘,2‘‘-terpyridine)]$^{2+}$ conjugated to a similar polymer backbone, redox potential of +0.55 V vs Ag/AgCl, as mediators. The cell was studied under conditions appropriate for high activity of the laccase enzyme: aerated pH 5 citrate buffer and chloride free medium containing 15 mM glucose. Maximum power density reached 137 μWcm^{-2} at 37 °C. The power dropped by less than 10% after a day of continuous operation and by 25% after three days. The cell power output was then refined [41] by the use of an anodic redox polymer with a more appropriate redox potential of −0.29 V and a flexible tether to improve charge transport diffusion. In this case a [Os(N,N‘-alkylated-2,2‘-biimidazole)$_3$]$^{2+}$ redox active moiety was tethered to the polymer backbone via one of its alkylated biimidazole ligands through a 13-atom long flexible spacer. At 37 °C the maximum power density for the cell was 268 μWcm^{-2} at 0.78 V. Under continuous operation for a week at 0.78 V and 37 °C the cell power dropped by 10% a day. The same refinement procedure was followed for the cathode [94], where a [Os(4,4‘-dimethyl-2,2‘-bipyridine)$_2$(4-aminomethyl-4‘-methyl-2,2‘-bipyridine)]$^{2+}$ complex was reacted with partially quaternized polyvinylpyridine to yield an 8-atom long flexible tether. The power density of this miniature biocatalytic fuel cell peaked (350 μWcm^{-2}) at 0.88 V, the highest cell voltage to date for a working miniature glucose-O_2 biocatalytic fuel cell, and just 300 mV below the thermodynamic potential of the glucose-O_2 cell reaction.

Along the principles just delineated above and almost concomitantly, the same group developed their own GOx-BOD fuel cell, for reasons already discussed. The refinement of the biocatalytic fuel cell was conducted in pseudo-physiological conditions of pH 7.4, 20 mM phosphate buffer containing 0.15 M NaCl and 15 mM glucose, air saturated solution with oxygen concentration ~ 0.2 mM at 37°C. In all cases the cathode redox polymer consisted of a polyvinylimidazole-polyacrylamide co-polymer functionalized with [Os(4,4’-dichloro-2,2’-bipyridine)$_2$Cl]$^+$, redox potential of +0.35 V vs. Ag/AgCl. The anode redox polymer was initially [Os(4,4’-diamino-2,2’-bipyridine)$_2$Cl]$^+$, redox potential of −0.16 V vs. Ag/AgCl, complexed to a partially quaternized polyvinylimidazole [81]. The assembled biocatalytic fuel cell power density was 50 μWcm^{-2} at 0.5 V. Two days of continuous operation resulted in 40% loss of the initial power density. Using a redox polymer containing [Os(4,4’-dimethoxy-2,2’-bipyridine)$_2$Cl], with a slightly more anodic potential of −0.07 V vs Ag/AgCl, for the anode [95], the maximum power density increased significantly to 244 μWcm^{-2} at the lower voltage of 0.36 V. This illustrates the limiting effect of the anode on the biocatalytic fuel cell performance under these conditions. One day of continuous operation of this cell resulted in less than 10% loss at 0.36 V, and 45% loss after four days. Further refinement of the anode involved, as was the case for the GOx-laccase fuel cell, introduction of a long flexible spacer between the polymer and [Os(N,N‘-alkylated-2,2‘-biimidazole)$_3$]$^{2+/3+}$ redox active moiety to improve diffusional charge transport between the enzyme active site and the electrode [96]. Despite the lowering of the redox potential to −0.19 V vs. Ag/AgCl, the cell produced a power density of 430 μWcm^{-2} at the relatively high voltage of 0.52 V. One week of continuous

operation at 0.52 V, resulted in a ~ 6% loss in power density per day. The operation of this cell in a living plant has been demonstrated [97]. A grape sap was chosen for its high glucose content (>30mM). The biocatalytic fuel cell performance depended on O_2 transport. In the O_2-deficient grape center the power density was 47 μWcm^{-2} whereas near the better oxygenated grape skin it reached 240 μWcm^{-2}, with an operating voltage of 0.52 V for both cases. Further improvement in output for this biofuel cell was achieved by increasing the redox site density of the anode redox polymer, resulting in a glucose flux-limited current density increase of 20% and an overpotential decrease of 50 mV [98]. This optimized biocatalytic fuel cell operated at +0.60 V with a 480 μWcm^{-2} power density in pH 7.2 phosphate buffer containing 0.1 M NaCl, 15 mM glucose at 37.5 °C, losing about 8% of its power each day of operation.

12.7. Conclusions

It seems that using and developing the different strategies discussed above, biocatalytic fuel cells with power densities and operating voltage high enough to power low-energy microdevices are now at hand. Indeed, a tremendous improvement has been shown from the initial units of μWcm^{-2} for the cell power density and tens of millivolts for the operating voltage, to achieve outputs approaching $mWcm^{-2}$ and operating voltages of ~0.5 V. Biocatalytic fuel cell optimization to date has mostly dealt with attempts to achieve direct electron transfer to the biocatalyst, and with matching the redox potential of the mediator with the biocatalytic elements. An important factor to consider, addressed by some, in the biocatalytic fuel cell refinement process is the nature of the electrode. The introduction of solid nanoparticles and fibers, for example of gold or carbon, in the biocatalytic electrodes can further improve current and power densities, whilst opening up the possibility of direct electron transfer with the biocatalytic active site.

A remaining crucial technological leap to pass for an implanted device remains the stability of the biocatalytic fuel cell, that should be expressed in months or years rather than days or weeks. Recent reports on the use of BOD biocatalytic electrodes in serum have, for example, highlighted instabilities associated with the presence of O_2, urate or metal ions [99,100], and enzyme deactivation in its oxidized state [101]. Strategies to be considered include the use of new biocatalysts with improved thermal properties, or stability towards interferences and inhibitors, the use of nanostructured electrode surfaces and chemical coupling of films to such surfaces, to improve film stability, and the design of redox mediator libraries tailored towards both mediation and immobilization.

12.8. References

[1] A. Heller, AIChE Journal, 51 (2005) 1054.
[2] Useful reviews for an introduction to this area are: (a) S. C. Barton, J. Gallaway, P. Atanassov, Chem. Rev., 104 (2004) 4867. (b) E. Katz, A. N. Shipway, I. Willner, In : Handbook of Fuel Cells – Fundamentals, Technology and Applications, W. Vielstich, H.A. Gasteiger, A. Lamm, Eds., Vol. 1, Chapter 21, Biochemical fuel cells, John Wiley & Sons, Ltd. 2003 (c) K. Rabaey, W. Verstraete Tr. Biotechnol. 23 (2005) 91.
[3] A. Heller, Phys. Chem. Chem. Phys., 6 (2004) 209.

[4] A. T. Yahiro, S. M. Lee, D. O. Kimble, Biochim. Biophys. Acta, 88 (1964) 375.
[5] H. A. O. Hill, Coord. Chem. Rev., 151 (1996) 115.
[6] J. Kim, H. Jia, P. Wang, Biotechnol. Advances, 24 (2006) 296.
[7] R.A. Bullen, T.C. Arnot, J.B. Lakeman, F.C. Walsh, Biosens. & Bioelectron., 21 (2006) 2015.
[8] S. Shleev, J. Tkac, A. Christenson, T. Ruzgas, A. I. Yaropolov, J. W. Whittaker, L. Gorton, Biosens. Bioelectron., 20 (2005) 2517.
[9] S. Shleev, A. Jarosz-Wilkolazka, A. Khalunina, O. Morozova, A. Yaropolov, T. Ruzgas, L. Gorton Bioelectrochem., 67 (2005) 115.
[10] S. Tsujimura, K. Kano, T. Ikeda, J. Electroanal. Chem., 576 (2005) 113.
[11] W. Zheng, Q. F. Li, L. Su, Y. M. Yan, J. Zhang, L. Q. Mao, Electroanal., 18 (2006) 587.
[12] Y. Liu, M. K. Wang, F. Zhao, Z. A. Xu, S. Dong, Biosens. & Bioelectron. 21 (2005) 984.
[13] C. Cai, J. Chen, Anal. Biochem., 332 (2004) 75.
[13] I. Willner, V. Heleg-Shabtai, R. Blonder, E. Katz, G. Tao, A. F. Buckmann, A. Heller, J. Am. Chem. Soc., 118 (1996) 10321.
[15] E. Katz, A. Riklin, V. Heleg-Shabtai, I. Willner, A. F. Buckmann, Anal. Chim. Acta, 385 (1999) 45.
[16] E. Katz, B. Filanovsky and I. Willner, New J. Chem., 23 (1999) 481.
[17] E. Katz, I. Willner, A.B. Kotlyar, J. Electroanal. Chem., 479 (1999) 64.
[18] F. Barrière, P. Kavanagh, D. Leech, Electrochim. Acta, 51 (2006) 5187.
[19] A. Pizzariello, M. Stred'ansky, S. Miertuš, Bioelectrochem., 56 (2002) 99.
[20] I. Willner, G. Arad, E. Katz, Bioelectroch. Bioener., 44 (1998) 209.
[21] I. Willner, E. Katz, F. Patolsky, A. F. Bückmann, J. Chem. Soc., Perkin Trans. 2 (1998) 1817.
[22] T. Ruzgas, A. Gaigalas, L. Gorton, J. Electroanal. Chem., 469 (1999) 123.
[23] T. Lotzbeyer, W. Schuhmann, H-L. Schmidt, Bioelectroch. Bioener., 42 (1997) 1.
[24] Z. Xu, N. Gao, H. Chen, S. Dong, Langmuir, 21 (2005) 10808.
[25] A. Ramanavicius, A. Kausaite, A. Ramanaviciene, Biosens. & Bioelectron. 20 (2005) 1962.
[26] G. T. R. Palmore, H-H. Kim, J. Electroanal. Chem., 464 (1999) 110.
[27] R. Bourbonnais, M. G. Paice, FEBS Letters, 267 (1990) 99.
[28] A.I. Yaropolov, O.V. Skorobogat'ko, S.S. Vartanov, S.D. Varfolomeyev, Appl. Biochem. Biotechnol., 49 (1994) 257.
[29] N. Duran, M. A. Rosa, A. D'Annibale, L. Gianfreda, Enz. Microb. Technol., 31 (2002) 907.
[30] F. Trudeau, F .Daigle, D. Leech, Anal. Chem., 69 (1997) 882.
[31] B. A. Kuznetsov, G. P. Shumakovich, O. V. Koroleva, A. I. Yaropolov, Biosens. & Bioelectron., 16 (2001) 73.
[32] Y. Ferry, D. Leech, Electroanal., 17 (2005) 113.
[33] R. Bourbonnais, M. G. Paice, D. Leech, Biochim. Biophys. Acta, 1379 (1998) 381.
[34] D. Rochefort, D. Leech, R. Bourbonnais, Green Chem., 6 (2004) 14.
[35] H. P. Call, I. Mucke, J. Biotech., 53 (1997) 163.
[36] E. Torres, I. Bustos-Jaimes, S. Le Borgne, Appl. Catal. B, 46 (2003), 1.

[37] S. C. Barton, H-H. Kim, G. Binyamin, Y. Zhang, A. Heller, J. Am. Chem. Soc., 123 (2001) 5802.
[38] T. Chen, S. C. Barton, G. Binyamin, Z. Q. Gao, Y. C. Zhang, H-H. Kim, A. Heller, J. Am. Chem. Soc., 123 (2001) 8630.
[39] S. C. Barton, H-H. Kim, G. Binyamin, Y. Zhang, A. Heller, J. Phys. Chem. B, 105 (2001) 11917.
[40] S. C. Barton, M. Pickard, R. Vazquez-Duhalt, A. Heller Biosens. & Bioelectron., 17 (2002) 1071.
[41] N. Mano, F. Mao, W. Shin , T. Chen, A. Heller, Chem. Comm. (2003) 518.
[42] F. Barrière, Y. Ferry, D. Rochefort, D. Leech, Electrochem. Comm., 6 (2004) 237.
[43] H. Yoshida, J. Chem. Soc., 43 (1883) 472.
[44] E. I. Solomon, U. M. Sundaram, T. E. Machonkin, Chem. Rev. 96 (1996) 2563.
[45] F. Xu, W. Shin, S. H. Brown, J. A. Wahleithner, U. M. Sundaram, E. I. Solomon, Biochim. Biophys. Acta, 1292 (1996) 303.
[46] F. Xu, H. J. W. Deussen, B. Lopez, L. Lam, K. C. Li, Eur. J. Biochem., 268 (2001) 4169.
[47] F. Xu, J. J. Kulys, K. Duke, K. C. Li, K. Krikstopaitis, H. J. W. Deussen, E. Abbate, V. Galinyte, P. Schneider, Appl. Env. Microbiol., 66 (2000) 2052.
[48] F. Xu, J. Biol. Chem., 272 (1997) 924.
[49] B. Reinhammer, Biochim. Biophys. Acta, 205 (1970) 35.
[50] I. V. Berezin, V. A. Bogdanovskaya, S. D. Varfolomeev, M. R. Tarasevich, A. I. Yaropolov, Dokl. Akad. Nauk SSSR, 240 (1978) 615.
[51] C. W. Lee, H. B. Gray, F. C. Anson, B. G. Malmstrom, J. Electroanal. Chem., 172 (1984) 289.
[52] M. H. Thuesen, O. Farver, B. Reinhammar, J. Ulstrup, Acta Chem. Scand. 52 (1998) 555.
[53] M. R. Tarasevich, V. A. Bogdanovskaya, A. V. Kapustin, Electrochem. Comm. 5 (2003) 491.
[54] C. Taylor, G. Kenausis, I. Katakis, A. Heller, J. Electroanal. Chem., 396 (1995) 511.
[55] D. Leech, K.O. Feerick, Electroanal., 12 (2000) 1339.
[56] S. Tsujimura, H. Tatsumi, J. Ogawa, S. Shimizu, K. Kano, T. Ikeda, J. Electroanal. Chem., 496 (2001) 69.
[57] S. Tsujimura, M. Kawaharada, T. Nakagawa, K. Kano, T. Ikeda, Electrochem. Comm., 5 (2003) 138.
[58] N. Mano, H-H. Kim, Y. Zhang, A. Heller, J. Am. Chem. Soc., 124 (2002) 6480.
[59] N. Mano, H-H. Kim, A. Heller, J. Phys. Chem., B, 106 (2002) 8842.
[60] N. Mano, J. L. Fernandez, Y. Kim, W. Shin, A. J. Bard, A. Heller, J. Am. Chem. Soc., 125 (2003) 15290.
[61] S. Tsujimura, K. Kano, T. Ikeda, J. Electroanal. Chem., 576 (2005) 113.
[62] M. T. Stankovich, L. M. Schopfer, V. Massey, J. Biol. Chem., 253 (1978) 4971.
[63] C. Godet, M. Boujtita, N. El Murr, New J. Chem., 23 (1999) 795.
[64] C. Cai, J. Chen, Anal. Biochem., 332 (2004) 75.
[65] J. H. T. Luong, S. Hrapovic, D. Wang, F. Benseba, B. Simard, Electroanal., 16 (2004) 132.

[66] J. Liu, A. Chou, W. Rahmat, M. N. Paddon-Row, J. J. Gooding, Electroanal., 17 (2005) 38.
[67] S. Liu, H. Ju, Biosens. & Bioelectron., 19 (2003) 177.
[68] F. Zhang, S. S. Cho, S. H. Yang, S. S. Seo, G. S. Cha, H. Nam, Electroanal., 18 (2006) 217.
[69] A. E. G. Cass, G. Davis, G. D. Francis, H. A. O. Hill, W. J. Aston, I. J. Higgins, E. V. Plotkin, L. D. Scott, A. P. F. Turner, Anal. Chem., 56 (1984) 667.
[70] N. J. Forrow, G. S. Sanghera, S. J. Walters, J. Chem. Soc. Dalton., (2002) 3187.
[71] S. M. Zakeeruddin, D. M. Fraser, M-K. Nazeeruddin, M. Grätzel, J. Electroanal. Chem., 337 (1992) 253.
[72] D. M. Fraser, S. M. Zakeeruddin, M. Grätzel J. Electroanal. Chem., 359 (1993) 125.
[73] Y. Liu, M. Wang, F. Zhao, B. Liu, S. Dong, Chem. Eur. J. 11 (2005) 4970.
[74] M. Zayats, E. Katz, I. Willner, J. Am. Chem. Soc., 124 (2002) 2120.
[75] F. Patolsky, Y. Weizmann, I. Willner, Angew. Chem. Int. Ed. 43 (2004) 2113.
[76] Y. Xiao, F. Patolsky, E. Katz, J. F. Hainfeld, I. Willner, Science 299 (2003) 1877.
[77] N. Mano, F. Mao, A. Heller, J. Electroanal. Chem., 574 (2005) 347.
[78] D. Leech, F. Daigle, Analyst, 123 (1998) 1971.
[79] T. Delumleywoodyear, P. Rocca , J. Lindsay, Y. Dror, A. Freeman, A. Heller, Anal. Chem., 67 (1995) 1332.
[80] H.-H. Kim, N. Mano, Y. Zhang, A. Heller, J. Electrochem. Soc., 150 (2003) A209.
[81] D. N. Blauch, J-M. Savéant, J. Phys. Chem., 97 (1993) 6444 and J. Am. Chem. Soc., 114 (1992) 3323.
[82] F. Mao, N. Mano, A. Heller, J. Am. Chem. Soc., 125 (2003) 4951.
[83] N. Mano, F. Mao, A. Heller, Chem. Commun., (2004) 2116.
[84] N. Yuhashi, M. Tomiyama, J. Okuda, S. Igarashi, K. Ikebukuro, K. Sode, Biosens. & Bioelectron., 20 (2005) 2145.
[85] L. Ye, M. Hiimmerle, A. J. J. Olsthoorn, W. Schuhmann, H-L. Schmidt, J. A. Duine, A. Heller, Anal. Chem., 65 (1993) 238.
[86] T. Ikeda, K. Kano, Biochim. Biophys. Acta, 1647 (2003) 121.
[87] S. Tsujimura, K. Kano, T. Ikeda, Electrochemistry, 70 (2002) 940.
[88] S. Igarashi, K. Sode, Mol. Biotechnol., 24 (2003) 97.
[89] F. Sato, M. Togo, M. K. Islam, T. Matsue, J. Kosuge, N. Fukasaku, S. Kurosawa, M. Nishizawa, Electrochem. Comm., 7 (2005) 643.
[90] Y. Ogino, K. Takagi, K. Kano, T. Ikeda, J. Electroanal. Chem., 396 (1995) 517.
[91] G. T. R. Palmore, H. Bertschy, S. H. Bergens, G. M.Whitesides, J. Electroanal. Chem., 443 (1998) 155.
[92] E. Simon, C. M. Halliwell, C. S. Toh, A. E. G. Cass, P. N. Bartlett, Bioelectrochem., 55 (2002) 13.
[93] C. M. Halliwell, E. Simon, C. S. Toh, A. E. G. Cass, P. N. Bartlett, Bioelectrochem., 55 (2002) 21.
[94] V. Soukharev, N. Mano, A. Heller, J. Am. Chem. Soc., 126 (2004) 8368.
[95] N. Mano, A. Heller, J. Electrochem. Soc., 150 (2003) A1136.
[96] N. Mano, F. Mao, A. Heller, J. Am. Chem. Soc., 124 (2002) 12962.
[97] N. Mano, F. Mao, A. Heller, J. Am. Chem. Soc., 125 (2003) 6588.
[98] N. Mano, F. Mao, A. Heller, ChemBioChem, 5 (2004) 1703.

[99] G. Binyamin, T. Chen, A. Heller, J. Electroanal. Chem., 500 (2001) 604.
[100] C. Kang, H. Shin, Y. Zhang, A. Heller, Bioelectrochem., 65 (2004) 83.
[101] C. Kang, H. Shin, A. Heller, Bioelectrochem., 68 (2006) 22.